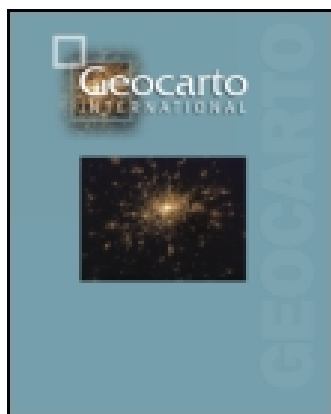


This article was downloaded by: [University of Tokyo]

On: 03 July 2014, At: 22:23

Publisher: Taylor & Francis

Informa Ltd Registered in England and Wales Registered Number: 1072954 Registered office: Mortimer House, 37-41 Mortimer Street, London W1T 3JH, UK



Geocarto International

Publication details, including instructions for authors and subscription information:

<http://www.tandfonline.com/loi/tgei20>

Characterization of forests and deforestation in Cambodia using ALOS/PALSAR observation

Ram Avtar ^a , Haruo Sawada ^a , Wataru Takeuchi ^a & Gulab Singh ^b

^a Institute of Industrial Science , The University of Tokyo , 4-6-1 Komaba, Meguro-Ku, Tokyo , 153-8505 , Japan

^b Graduate School of Science and Technology , Niigata University , Niigata , 950-2181 , Japan

Accepted author version posted online: 23 Sep 2011. Published online: 20 Oct 2011.

To cite this article: Ram Avtar , Haruo Sawada , Wataru Takeuchi & Gulab Singh (2012) Characterization of forests and deforestation in Cambodia using ALOS/PALSAR observation, Geocarto International, 27:2, 119-137, DOI: [10.1080/10106049.2011.626081](https://doi.org/10.1080/10106049.2011.626081)

To link to this article: <http://dx.doi.org/10.1080/10106049.2011.626081>

PLEASE SCROLL DOWN FOR ARTICLE

Taylor & Francis makes every effort to ensure the accuracy of all the information (the "Content") contained in the publications on our platform. However, Taylor & Francis, our agents, and our licensors make no representations or warranties whatsoever as to the accuracy, completeness, or suitability for any purpose of the Content. Any opinions and views expressed in this publication are the opinions and views of the authors, and are not the views of or endorsed by Taylor & Francis. The accuracy of the Content should not be relied upon and should be independently verified with primary sources of information. Taylor and Francis shall not be liable for any losses, actions, claims, proceedings, demands, costs, expenses, damages, and other liabilities whatsoever or howsoever caused arising directly or indirectly in connection with, in relation to or arising out of the use of the Content.

This article may be used for research, teaching, and private study purposes. Any substantial or systematic reproduction, redistribution, reselling, loan, sub-licensing, systematic supply, or distribution in any form to anyone is expressly forbidden. Terms &

Conditions of access and use can be found at <http://www.tandfonline.com/page/terms-and-conditions>

Characterization of forests and deforestation in Cambodia using ALOS/PALSAR observation

Ram Avtar^{a*}, Haruo Sawada^a, Wataru Takeuchi^a and Gulab Singh^b

^a*Institute of Industrial Science, The University of Tokyo, 4-6-1 Komaba, Meguro-Ku, Tokyo 153-8505, Japan;* ^b*Graduate School of Science and Technology, Niigata University, Niigata 950-2181, Japan*

(Received 15 July 2011; final version received 12 September 2011)

In this study, we have demonstrated the capability of full polarimetric ALOS/Phased Array L-band Synthetic Aperture Radar data for the characterization of the forests and deforestation in Cambodia, to support climate change mitigation policies of Reducing Emission from Deforestation and Forest Degradation (REDD). We have observed mean backscattering coefficient (σ°), entropy (H), alpha angle (α), anisotropy (A), pedestal height (PH), Radar Vegetation Index (RVI) and Freeman–Durden three-component decomposition parameters. The observations show that the forest types and deforested area are showing variable polarimetric and backscattering properties because of the structural difference. Evergreen forest is characterized by a high value of σ° HV (−12.96 dB) as compared with the deforested area (σ° HV = −22.2 dB). The value of polarimetric parameters such as entropy (0.93), RVI (0.91), PH (0.41) and Freeman–Durden volume scattering (0.43) is high for evergreen forest, whereas deforested area is characterized by the low values of entropy (0.36) and RVI (0.17). Based on these parameters, it is found that σ° HV, entropy, RVI and PH provide best results among other parameters.

Keywords: deforestation; PALSAR; backscattering coefficient (σ°); RVI; pedestal height; REDD

1. Introduction

Forests have a vital socio-economic and environmental importance and play an important role in maintaining ecological balance and homeostatic in the environment (Lackey 1998). The tropical forests play a crucial role in the global carbon cycle, acting as a carbon sink and source of atmospheric carbon dioxide (CO₂). They are habitat for about two-thirds of the Earth's terrestrial biodiversity. They also provide a significant benefit to humans at the local and global scales (Gardner *et al.* 2009). Recent reports indicate that deforestation caused a loss of about 13 million hectares (ha) of tropical forests area per year from the year 2000 to 2010 (Achard *et al.* 2010, FRA 2010). The deforestation and forest degradation contribute to the emission of more than 17% green house gases (GHGs) and are the second largest source, after the fossil fuels (Gibbs and Herold 2007, IPCC 2007, Schrope 2009, Werf *et al.* 2009) which is a consequence of the rapid economic growth, increasing demand for agricultural land, forestry products, illegal logging and urbanization

*Corresponding author. Email: ram.envjnu@gmail.com

(Rudel *et al.* 2009). Hence, there is a need to reduce deforestation and forest degradation, as it is adversely impacting the carbon cycle, climate and biodiversity. For the proper estimation of the emissions of GHGs from deforestation and forest degradation in a developing country, information of the spatial distribution of forest types and the changes in the forest cover are needed.

Reducing Emission from Deforestation and Forest Degradation (REDD) is an United-Nations endorsed mechanism to mitigate climate change by assisting the developing countries for making strategies for the reduction of deforestation and forest degradation through implementing community forestry (REDD 2010). For the implementation of REDD policies, an accurate assessment of (a) place of deforestation with forest types, (b) aerial extent (hectares), (c) biomass lost (percentage), (d) carbon contents in each forest type (metric tons of carbon per hectare) and (e) the process of forest loss is needed (Ramankutty *et al.* 2007).

The traditional field-based assessment of the forest distribution is a tedious, expensive and time-consuming process, especially, making an assessment at a large scale in remote areas (Knuth *et al.* 2009). Remote sensing is a useful tool to monitor the distribution of forest at various spatial and temporal scales, when combined with the ground truth data. Remote sensing technique is also an advantageous tool due to its repetitive measurements at a large-scale synoptic view (Lu 2006, Avtar *et al.* 2011). Currently, most of the operational systems used for deforestation monitoring are based on the optical sensors (Gibbs *et al.* 2007). However, launching of the synthetic aperture radar (SAR)-based satellites (e.g. JERS, Phased Array L-band Synthetic Aperture Radar (PALSAR), RADARSAT-1/2, ERS-1/2, ENVISAT and TerraSAR-X) has opened a wide spectrum for regular and cloud-free observations in tropical regions (Kuntz 2010). SAR-based observations can provide information about dielectric properties, roughness, orientation, etc. of the objects. Most of the previous studies (Le Toan *et al.* 1992, Beaudoin *et al.* 1994, Dobson *et al.* 1995, Watanabe *et al.* 2006, Mitchard *et al.* 2009) have been done using SAR backscattering coefficient (σ°) as a main parameter for forest cover and deforestation monitoring. On the other hand, this study attempts to examine various other polarimetric parameters to characterize forests and deforestation in Cambodia. In this study, we used relative polarimetric descriptors, viz. Radar Vegetation Index (RVI), pedestal height (PH), H , α and A for the characterization of forest types and deforestation, as these polarimetric descriptors have minor effects from the topography, incidence angle and other calibration errors (Kim and van Zyl 2001).

Kiyono *et al.* (2010), using their model [total carbon stock = $\sum(\text{forest area}_i \times \text{average carbon stock}_i)$] (where i stands for forest types), estimates the emissions of CO₂ from deforestation. The implementation of this model needs an accurate monitoring of the forest types and deforestation. Our study is an attempt to develop a better understanding to discriminate forest types and deforestation based on the polarimetric behaviour of PALSAR so that effective implementation of REDD policies can be undertaken.

2. Study area

Cambodia is a tropical country covered with about 57% of tropical forest (FRA 2010). Cambodia has lost about 29% of primary forest between the year 2000 and 2005, which accumulates high biomass as compared with the other forest types (FRA 2005). Moreover, Cambodia has the highest annual deforestation rate among the

Indochina countries (FRA 2010). Cambodia also has a rainy season from May to October and dry season from November to April. The minimum and maximum temperature of the area is about 21°C and 35°C, respectively. The mean annual precipitation varies from 150 to 180 cm. Figure 1 shows the study area (about 1880 km²) situated in Stung Treng and Kratie province of northern Cambodia.

3. Methodology

3.1. Satellite data

Two scenes of full polarimetric (HH, HV, VH and VV) 1.1 level PALSAR data were acquired on 17 May 2007 and 6 April 2009 with 21.5° look angle. Data from the Landsat Thematic Mapper (TM5) and AVNIR-2 were acquired in June 2006 and March 2010, respectively, and were used for the selection of forest cover types. High-resolution (2.5 m) PRISM data acquired on November 2009 with the nadir and backward look angle were also used for the selection of the area of interest (AOI). Along with satellite data, field-based experience was also used for the selection of AOIs.

3.2. Land use/land cover map

AVNIR-2 data acquired in March 2010 were used to generate land cover map of the area supported with ground truth data. Field collected data along with field-based experience have been used for the selection of training samples. Land cover map (Figure 2) was generated using supervised method with the maximum likelihood classification (MLC) technique. The study area was classified into seven land cover classes, viz. evergreen forest, deciduous forest, sparsely deciduous forest, wood and shrub land, deforested area and agricultural land and water. Most of the area is covered by the evergreen forest followed by the deciduous forest, sparsely deciduous forest and other classes. Table 1 shows the percentage of different land cover classes of the area.

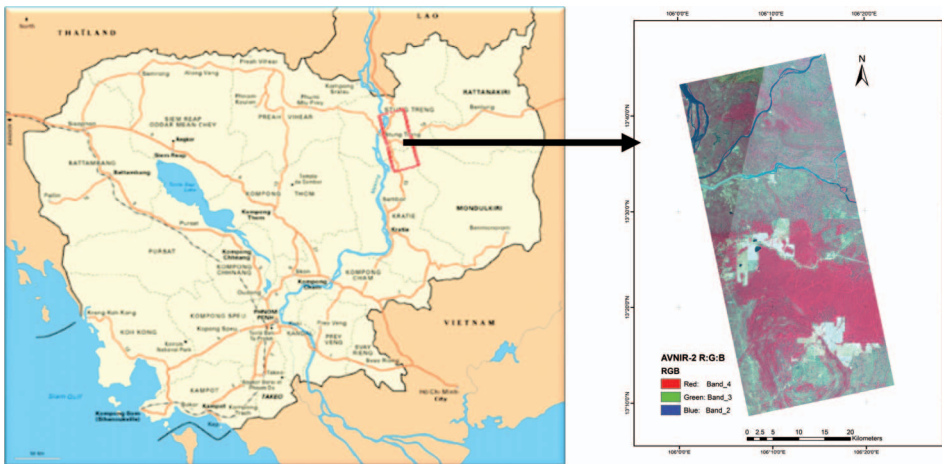


Figure 1. Location of the study area.

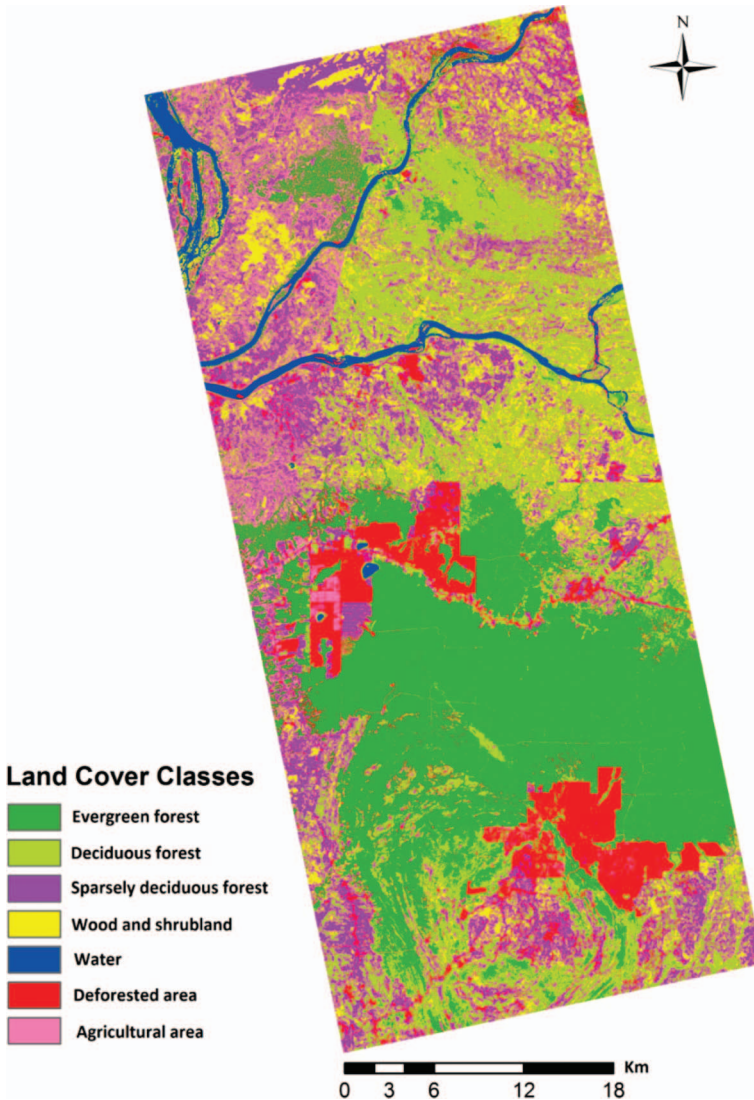


Figure 2. Land cover map of the area (based on MLC of AVNIR-2 March 2010 data).

3.3. Field data

The primary data, such as forest types, species, diameter at breast height (DBH), tree height and tree density, are essential for carbon stock estimation. These forest inventory data were collected on the basis of stratified random sampling during December 2009 and January 2011. The homogeneous site has been selected on the basis of analysis of above-mentioned satellite data. Four plots of evergreen forest, four plots of deciduous and three plots of sparsely deciduous forest were selected for forest inventory data. The 30×60 -m and 30×30 -m plots' size has been selected on the basis of position and homogeneity of the site. The GPS positions and GPS photos of en route forest cover types were also collected for further selection of the

plots for quantitative analysis. The biomass of the sampling plots has been calculated using Kiyono *et al.*'s (2010) allometric equation. Table 2 summarizes the details of forest inventory data.

3.4. Data processing

For the processing of PALSAR data-NEST, PolSARpro and ENVI software were used. The PALSAR images were calibrated radiometrically through converting the digital number to the normalized radar cross section in a decibel. The formula is given below (Shimada *et al.* 2009):

$$\sigma^o = 10 \times \log_{10}(I^2 + Q^2) + CF - 32.0 \quad (1)$$

where CF is calibration factor (CF = -86 dB) and I and Q are the real and imaginary parts of the complex SAR image pixel values, respectively. PALSAR 1.1 level full polarimetric, single look complex data were multi-looked at one time in range and six times in azimuth direction, converted from the slant to ground range so that the spatial resolution is reduced to nearly 21 m \times 23 m (azimuth \times range). Later, the data were filtered using Frost filter with a window size of 5 \times 5 to reduce speckle effects. All images were geo-referenced within pixel accuracy.

Table 1. Percentage of different types of land cover.

| Land cover classes | AVNIR-2-based classes | |
|---------------------------|-------------------------|----------------|
| | Area (km ²) | Land cover (%) |
| Evergreen forest | 550.1 | 29.7 |
| Deciduous forest | 388.1 | 21.0 |
| Sparsely deciduous forest | 387.8 | 20.9 |
| Wood and shrub land | 245.3 | 13.2 |
| Water body | 38.4 | 2.1 |
| Deforested area | 161.0 | 8.7 |
| Agricultural land | 81.4 | 4.4 |
| Total | 1852.1 | 100 |

Table 2. Forest inventory data for various forests.

| No. | Forest types | Mean height (m) | Mean DBH (cm) | Tree density (no./ha) | Plot size (ha) | Biomass (tons/ha) |
|-----|----------------------|-----------------|---------------|-----------------------|----------------|-------------------|
| 1 | Evergreen_1 | 20.32 | 21.96 | 544 | 0.18 | 254 |
| 2 | Evergreen_2 | 18.3 | 25.39 | 338 | 0.18 | 480 |
| 3 | Evergreen_3 | 17 | 19.7 | 532 | 0.09 | 170.5 |
| 4 | Evergreen_4 | 15.4 | 19.3 | 577 | 0.09 | 166.2 |
| 5 | Deciduous_1 | 7.49 | 20.94 | 311 | 0.18 | 102 |
| 6 | Deciduous_2 | 13.5 | 19.7 | 577 | 0.09 | 149 |
| 7 | Deciduous_3 | 12 | 21.6 | 288 | 0.09 | 141 |
| 8 | Deciduous_4 | 11 | 21.4 | 400 | 0.09 | 121.5 |
| 9 | Sparsely deciduous_1 | 10.5 | 20.6 | 222 | 0.09 | 58.7 |
| 10 | Sparsely deciduous_2 | 11.6 | 26.1 | 188 | 0.09 | 86 |
| 11 | Sparsely deciduous_3 | 10.34 | 25.53 | 166 | 0.18 | 73 |

The PALSAR data were analysed to represent different types of image regions, representing the different types of forest cover classes. An AOI was selected in homogeneous area on the basis of land cover map (Figure 2) and ground truth information (Table 2). The 40 AOIs were selected to analyse different types of polarimetric behaviour of PALSAR data. The selected AOIs were 12, 10, 9 and 9 in evergreen, deciduous, sparsely deciduous forests and deforested areas, respectively. The different polarimetric behaviours of the PALSAR data were analysed for each selected forest cover classes (AOI). Figure 3 represents

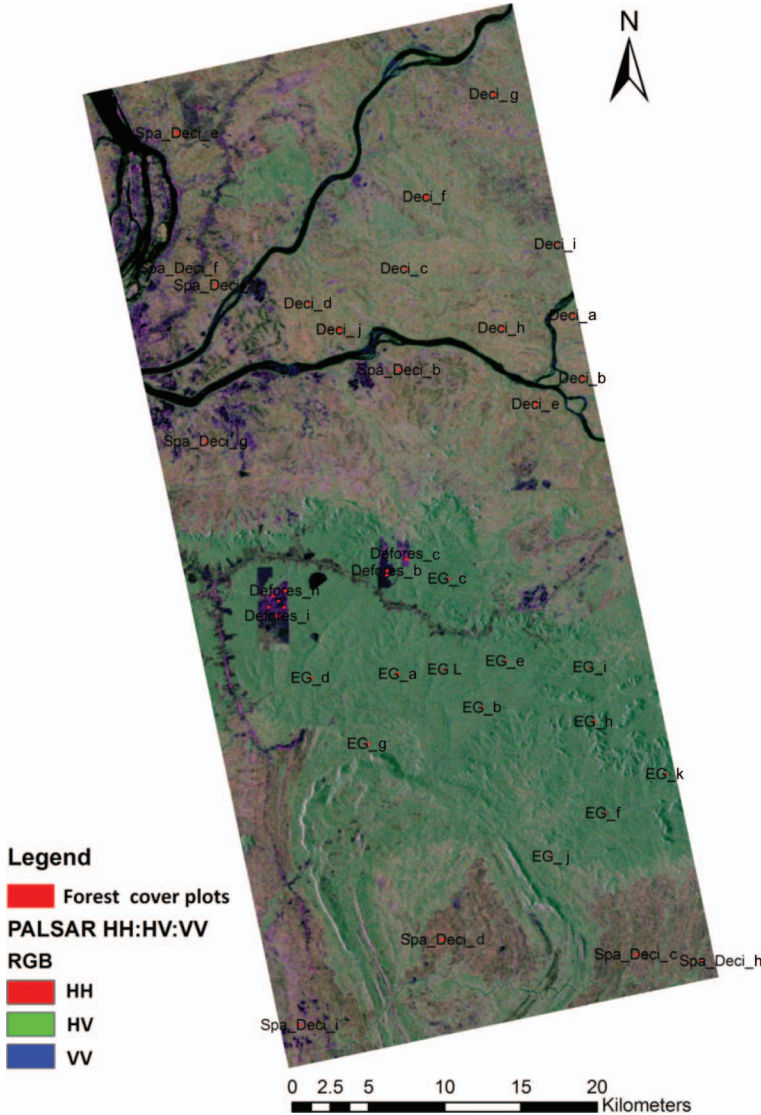


Figure 3. PALSAR (R:HH, G:HV, B:VV) data with the location of the sampling plots of different types of forest cover classes (EG is evergreen forest, Deci is deciduous forest, Spa_Dece is sparsely deciduous forest, Defores is deforested area and a, b, c, d, ... are the plot IDs of particular forest class).

PALSAR data with the location of the sampling plots (AOI) of different types of forests. Figure 4 shows the methodology adopted in this study. The backscattering (σ^0) properties depend on the target characteristics. It shows surface, volume and double bounce backscattering behaviours of the targets.

3.5. Polarimetric decomposition parameters

Polarimetric decomposition provides information to understand the physical characteristics of various scatterers. It is based on the eigenvalues and eigenvectors (Cloude and Pottier 1997). The entropy (H), alpha (α) angle and anisotropy (A) are polarimetric features and gives the information about scattering properties from the targets. Entropy is a measure that indicates the randomness of the scatterers. Zero

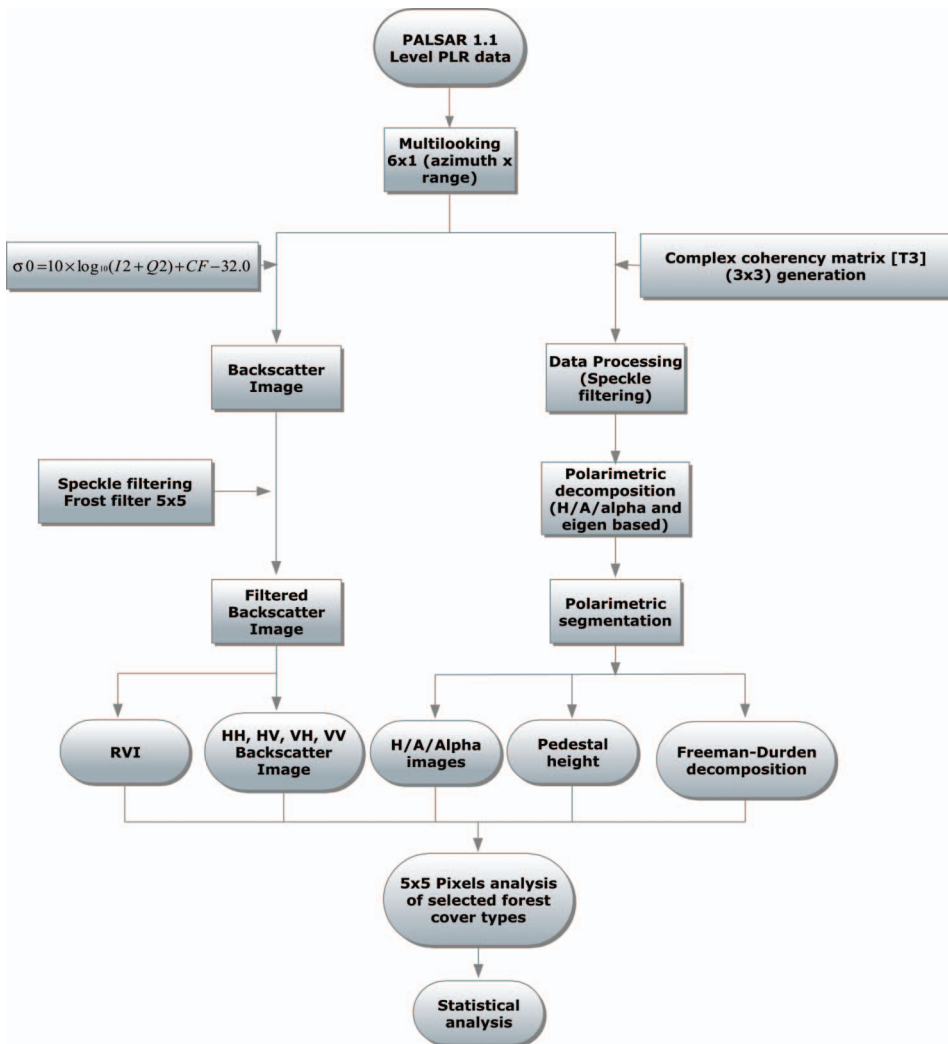


Figure 4. Flow chart of the methodology.

Downloaded by [University of Tokyo] at 22:23 03 July 2014

(0) value of H is for pure targets, whereas 1 for distributed targets (no dominant scatterers). H can be expressed as:

$$H = \sum_{i=1}^3 -P_i \log_3 P_i \quad (2)$$

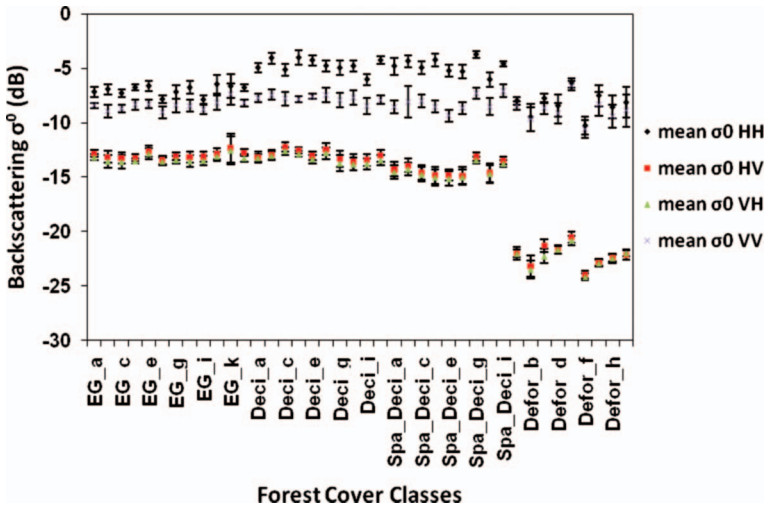


Figure 5. Graph represents the relation between PALSAR backscattering versus forest cover classes (EG is evergreen forest, Deci is deciduous forest, Spa_Deci is sparsely deciduous forest, Defor is deforested area and a, b, c, d . . . are the plot IDs of particular forest class).

Table 3. Statistical summary of polarimetric parameters for different types of forest.

| | Evergreen forest (mean \pm SD) | Deciduous forest (mean \pm SD) | Sparsely deciduous forest (mean \pm SD) | Deforested area (mean \pm SD) |
|-------------------------------|-------------------------------------|-------------------------------------|--|------------------------------------|
| σ° HH (dB) | -7.04 ± 0.46 | -4.73 ± 0.61 | -4.81 ± 0.68 | -8.29 ± 1.13 |
| σ° HV (dB) | -12.96 ± 0.34 | -12.99 ± 0.44 | -14.29 ± 0.63 | -22.25 ± 1.03 |
| σ° VH (dB) | -13.30 ± 0.34 | -13.27 ± 0.44 | -14.52 ± 0.59 | -22.42 ± 0.99 |
| σ° VV (dB) | -8.43 ± 0.44 | -7.78 ± 0.29 | -8.23 ± 0.71 | -8.86 ± 1.1 |
| σ° HH/HV (dB) | 5.95 ± 0.37 | 8.25 ± 0.65 | 9.48 ± 0.56 | 13.96 ± 0.6 |
| σ° HH/VV (dB) | 1.39 ± 0.36 | 3.05 ± 0.46 | 3.43 ± 0.65 | 0.57 ± 0.28 |
| Alpha ($^{\circ}$) | 46.25 ± 1.12 | 46.44 ± 1.3 | 43.03 ± 1.65 | 11.17 ± 1.8 |
| Entropy | 0.93 ± 0.01 | 0.85 ± 0.03 | 0.80 ± 0.03 | 0.36 ± 0.04 |
| Anisotropy | 0.12 ± 0.03 | 0.23 ± 0.05 | 0.26 ± 0.04 | 0.25 ± 0.05 |
| RVI | 0.91 ± 0.04 | 0.67 ± 0.06 | 0.54 ± 0.04 | 0.17 ± 0.02 |
| PH | 0.41 ± 0.03 | 0.26 ± 0.04 | 0.20 ± 0.02 | 0.04 ± 0.01 |
| Freeman–Durden_ surface | 0.03 ± 0.02 | 0.12 ± 0.06 | 0.22 ± 0.05 | 0.25 ± 0.08 |
| Freeman–Durden_ volume | 0.43 ± 0.03 | 0.42 ± 0.05 | 0.31 ± 0.05 | 0.04 ± 0.01 |
| Freeman–Durden_ double bounce | 0.01 ± 0.01 | 0.11 ± 0.06 | 0.05 ± 0.02 | 0.01 ± 0.002 |

where P_i is pseudo-probabilities, which can be obtained from the eigenvalues λ_i that represents relative intensity of the i th scattering process.

Alpha (α) is an angle based upon the eigenvectors and it measures the type of scattering from the targets. It varies from 0° to 90° . The value of α close to 0° , 45° and 90° represents the single bounce scattering from flat surfaces, volume scattering and double bounce scattering, respectively. Change in the value of α shows change in scattering properties of targets.

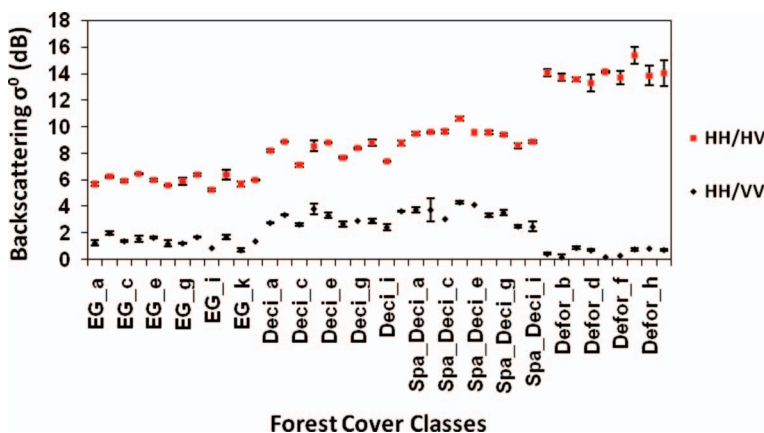


Figure 6. Variations in the cross-polar and co-polar ratios with forest cover classes.

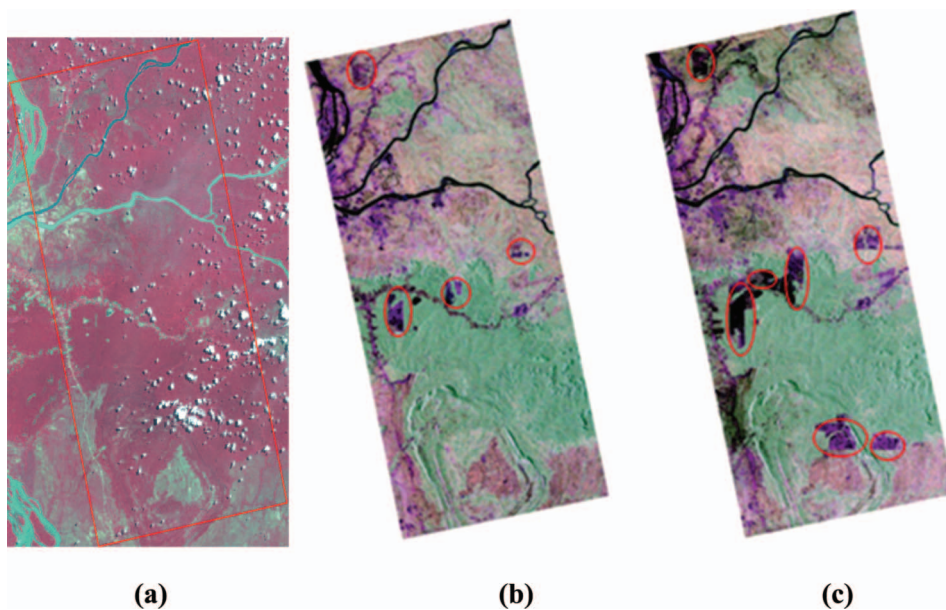


Figure 7. (a) Landsat TM image of 8 June 2006, (b) PALSAR (R:HH, G:HV, B:VV) image of 17 May 2007 and (c) PALSAR (R:HH, G:HV, B:VV) image of 6 April 2009. Red circle is showing deforested area.

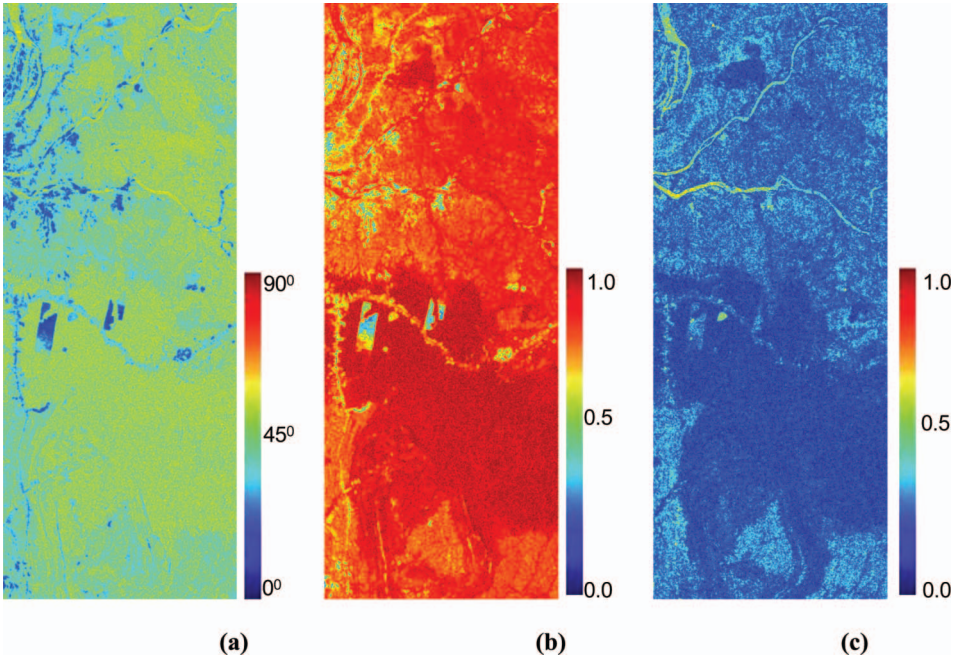


Figure 8. (a) Alpha, (b) entropy and (c) anisotropy images from PALSAR data.

$$\bar{\alpha} = \sum_{i=1}^3 P_i \alpha_i \quad (3)$$

Anisotropy (A) is a complementary parameter for entropy (H). Anisotropy measures the relative importance of the second and third eigenvalues of eigen decomposition. It can be used as a source of discrimination, when $H > 0.7$ (Fang *et al.* 2006, Trisasongko 2010).

$$A = \frac{\lambda_2 - \lambda_3}{\lambda_2 + \lambda_3} \quad (4)$$

where λ_2 and λ_3 are the smaller eigenvalues.

3.6. Radar Vegetation Index

RVI is used for analysing the scattering from the vegetated area showing high value of volume scattering targets (leaves, branches, etc.; Qi *et al.* 2010). Woody vegetation, having high cross-polarization components shows high values of RVI. RVI is derived from the radar backscattering coefficient (σ°) of HH, HV and VV polarizations (Kim and van Zyl 2001).

$$\text{RVI} = 8\sigma^\circ \text{HV} / \sigma^\circ \text{HH} + \sigma^\circ \text{VV} + 2\sigma^\circ \text{HV} \quad (5)$$

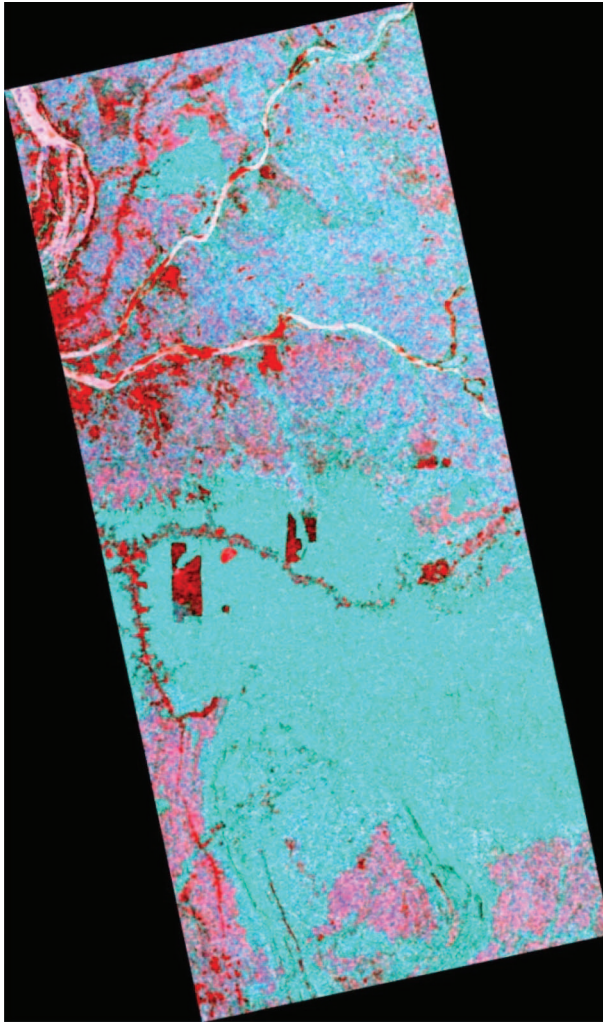


Figure 9. $H/A/\alpha$ (H -green; A -red; α -blue) colour image.

3.7. Pedestal height

PH is a used for measuring randomness in the scattering process. PH is simply a ratio of minimum eigenvalue (λ_3) to the maximum eigenvalue (λ_1). These eigenvalues correspond to the minimum and maximum powers achievable by optimizing over all antenna transmit and receive polarization (Lee and Pottier 2009). PH value varies from 0 to 1.

$$PH = \min(\lambda_1, \lambda_2, \lambda_3) / \max(\lambda_1, \lambda_2, \lambda_3) = \lambda_3 / \lambda_1 \quad \text{with } \lambda_3 \leq \lambda_2 \leq \lambda_1 \quad 0 \leq PH \leq 1 \quad (6)$$

3.8. Three-component target decomposition

Three-component scattering decomposition is a technique used for the fitting of a physically based three-component scattering mechanism model to polarimetric SAR data. Freeman and Durden decomposition (1998) is used to derive meaningful

information about the scatterers' characteristics (i.e. surface, volume and double bounce scattering). These surface, volume and double bounce scattering mechanisms are useful for the discrimination of various forest types and deforested area (Lee and Pottier 2009).

4. Results and discussion

Figure 5 shows the variations of mean backscattering coefficients (σ°) of HH, HV, VH and VV with different types of forest classes. The value of σ° depends on the polarization types. HH, HV and VV polarization represent surface scattering, canopy scattering and ground-trunk scattering, respectively, in the forest areas (Le Toan *et al.* 1992). These three scattering mechanisms are dependent on the polarimetry of forest types. The L-band backscattering coefficients have shown a good correlation with biophysical parameters (biomass and height) of the forest.

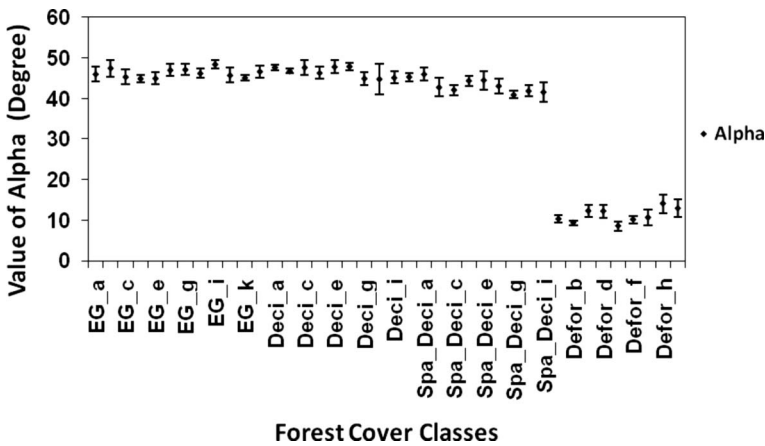


Figure 10. Variations of the alpha (α) angle with forest cover classes.

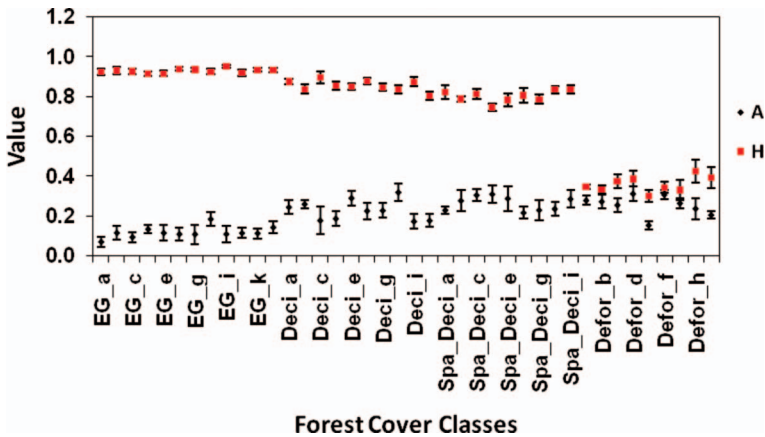


Figure 11. Variations of the entropy (H) and anisotropy (A) with forest cover classes.

Similar features have been observed at various locations for different types of forests (Le Toan *et al.* 1992, Beaudoin *et al.* 1994, Dobson *et al.* 1995, Watanabe *et al.* 2006, Mitchard *et al.* 2009). Table 3 illustrates the statistical summary of the observed polarimetric parameters for different types of forests. The mean σ° HV observed for evergreen, deciduous, sparsely deciduous forests and deforested area were -12.96 , -12.99 , -14.29 and -22.25 dB, respectively. The σ° HV of evergreen forest was comparatively higher than those observed for the other forest types (Table 3). This observed feature from evergreen forest was due to the fact that evergreen forest with multiple canopy enhances the volume scattering. The mean value of σ° HV backscattering for deciduous forest was higher compared with the sparsely deciduous forest and deforested area. This observation shows a saturation stage of

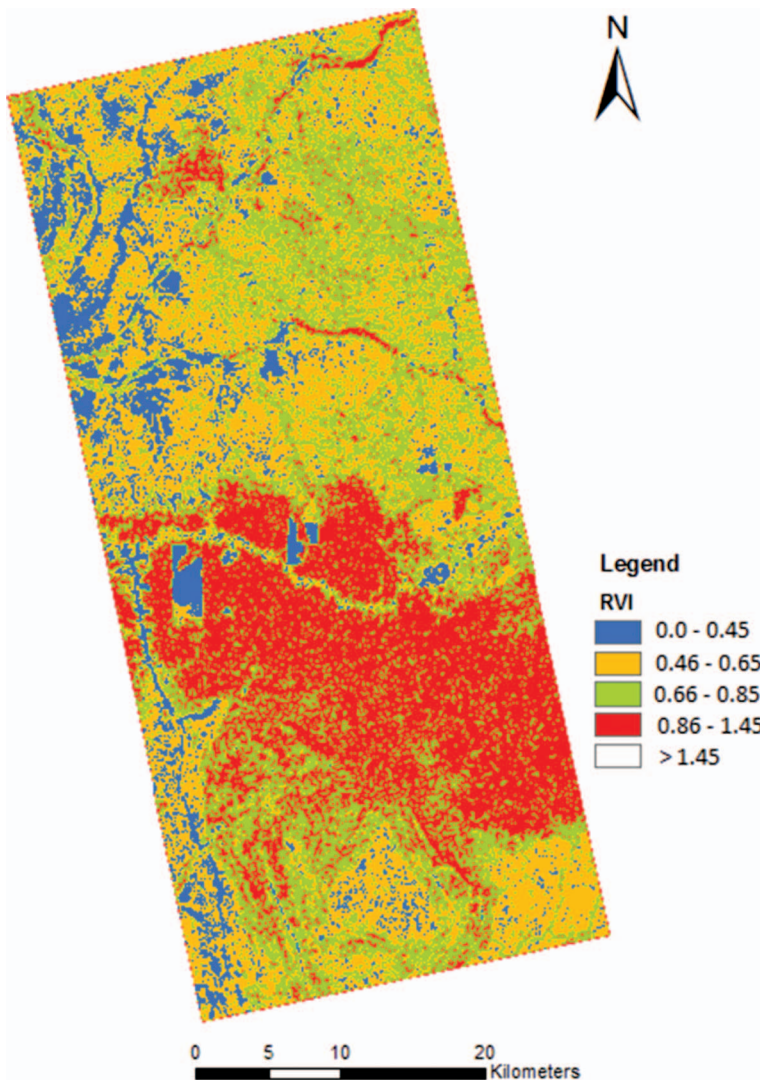


Figure 12. RVI image of the study area.

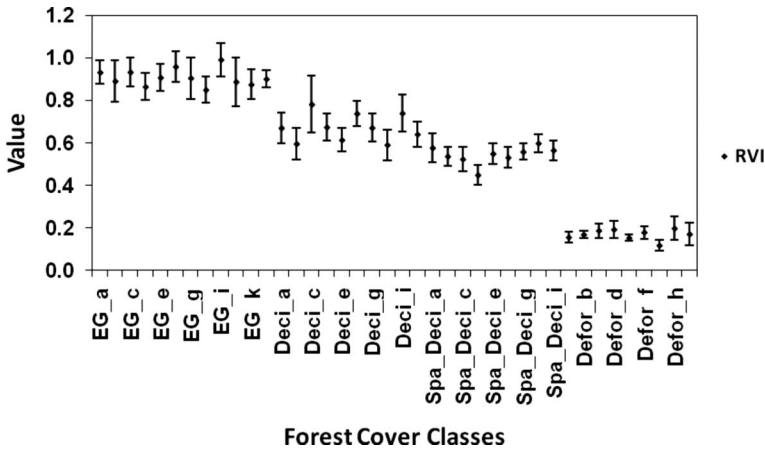


Figure 13. Variations of the RVI with forest cover classes.

the σ° HV, because deciduous forest has biomass greater than 100 tons/ha, which is a saturation limit of the σ° HV for PALSAR. Watanabe *et al.* (2006) has also found saturation of PALSAR signal at 100 tons/ha. The observed mean σ° HH shows a higher value for deciduous and sparsely deciduous forests, whereas lower for evergreen (Table 3). This is due to the higher penetration of L-band (low incidence angle 23.1°) which caused surface scattering. The value of mean σ° HV is very low for deforested area due to the absence of volume scattering. The mean σ° HH for some deforested plot has shown a higher value in the recent cutover forest, but it decreases over a period of time. This high value of σ° HH in recent deforested area might be because of the presence of wooden logs, which increases surface roughness (Isoguchi *et al.* 2009). Therefore, in case of deforested area, the σ° HV shows a sudden change as compared with σ° HH.

Figure 6 shows the variations of HH/HV polarization ratio with different types of forest classes, and the observed values of HH/HV are illustrated in Table 3. The mean value of the HH/HV polarization ratio was lower for evergreen forest (5.95 dB) than those observed for deciduous (8.25 dB) and sparsely deciduous forests (9.48 dB). On the other hand, the HH/HV polarization ratio observed for the deforested area is highest (13.96 dB). The variations of HH/VV co-polarization ratio are high for deciduous (3.05 dB) and sparsely deciduous forests (3.43 dB), whereas lower for evergreen forests (1.39 dB). In case of the deforested area, the value of HH/VV co-polarization ratio is slightly low (0.57 dB). Hence, the HH/HV (cross-polarization) polarization ratio is better than HH/VV (co-polarization ratio) to identify the type of forests and deforestation because of the 2- to 4-dB difference in backscattering.

Figure 7(a) shows the false colour composite of the Landsat TM5 data of June 2006, while Figure 7(b) and (c) shows R:HH, G:HV, and B:VV colour composite of the PALSAR backscatter images observed during May 2007 and April 2009. From the comparison of the images in Figure 7(a)–(c), it can be estimated that the area of cutover forest of about 20.13 km² and 43.32 km², occurred from the years 2006 to 2007 and 2007 to 2009, respectively. The entropy (H), alpha angle (α) and anisotropy (A) images from PALSAR data have been generated using eigenvalue-based target

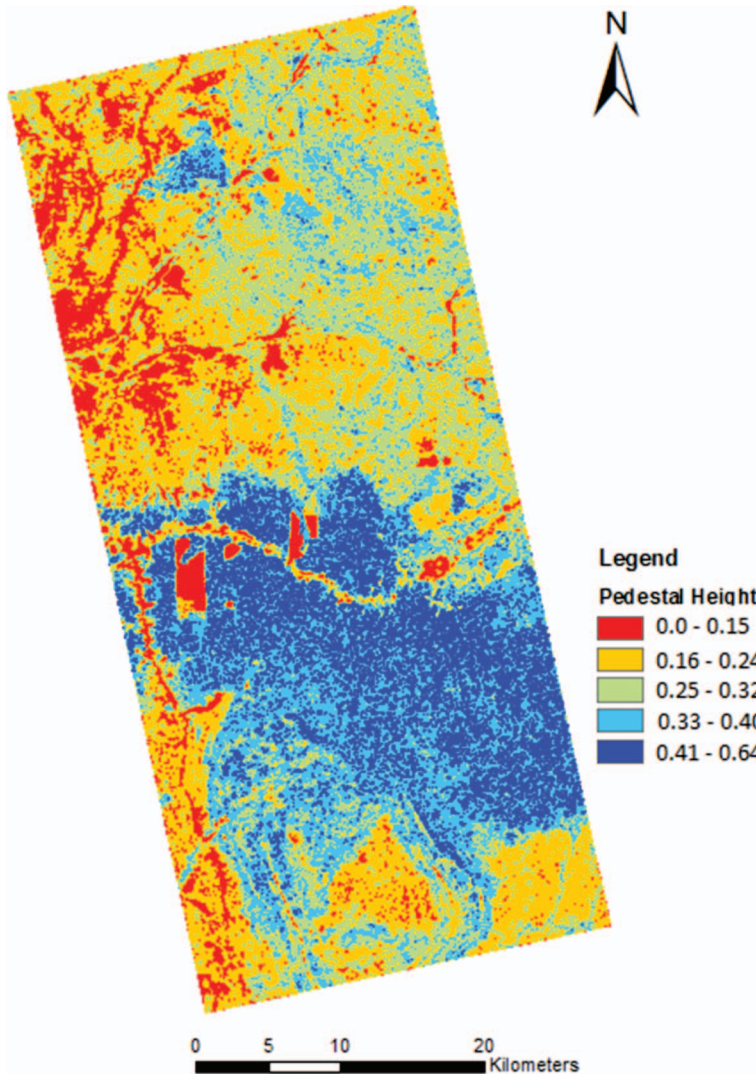


Figure 14. PH image of the study area.

decomposition (Figure 8(a)–(c)). The H -, α - and A -based R:G:B colour composite is shown in Figure 9. The value of α ranges from 40° to 50° for evergreen, deciduous and sparsely deciduous forests. On the other hand, it decreases to 10 – 15° for deforested area due to surface scattering (Figure 10 and Table 3). The mean value of the entropy for evergreen forest is higher (0.93) than those shown by deciduous (0.85) and sparsely deciduous (0.80) forest (Figure 11). Forests show a high value of entropy because of the distributed targets, which causes depolarization effects due to the volume scattering from the vegetation. The value of entropy becomes less for deforested area because most of the deforested area shows the pure target properties (Guerra *et al.* 2008). Therefore, decreasing the entropy can be regarded as

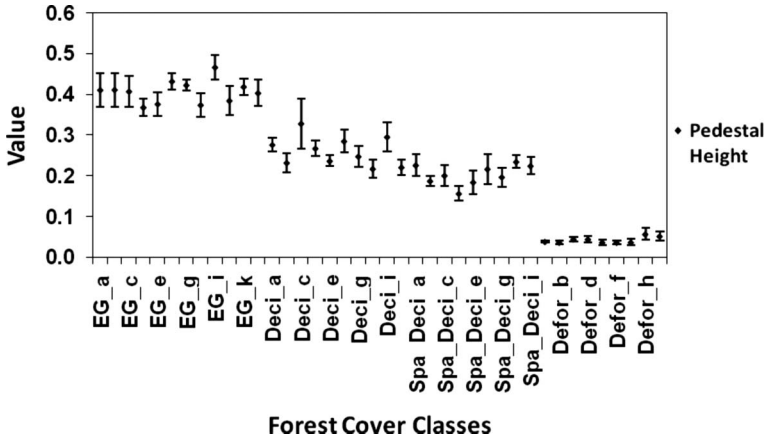


Figure 15. Variations of the PH with forest cover classes.

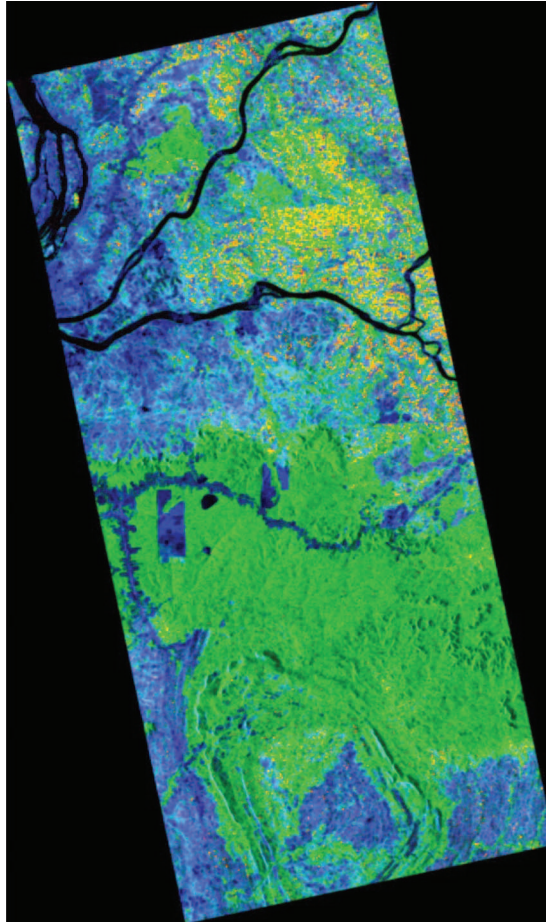


Figure 16. Freeman–Durden (R:double bounce scattering, G:volume scattering, B:surface scattering) image of PALSAR data.

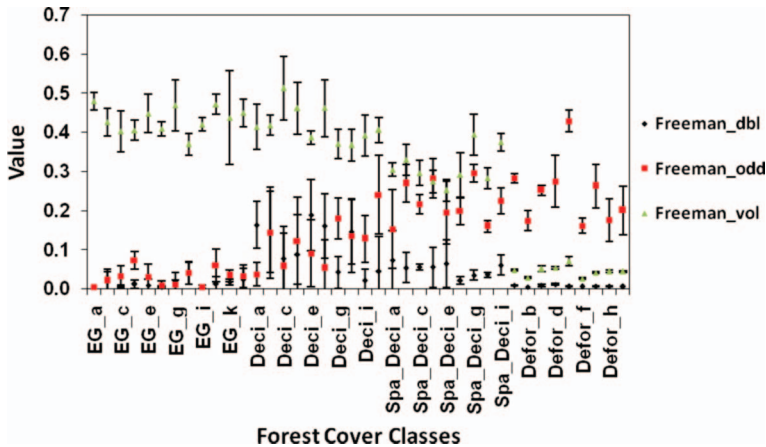


Figure 17. Variations of the Freeman scattering with forest cover classes.

deforestation. However, it should be confirmed by ground truth observation. The value of anisotropy shows small changes for deforested area (Figure 11).

Figure 12 shows the RVI image of the study area. The mean value of RVI is higher for evergreen forest (0.91) compared with those shown by deciduous (0.67) and sparsely deciduous (0.54) forests (Figure 13). High value of RVI in evergreen forest is because of the multi-story tree structure with complex canopy which causes high σ° in HV polarization. The RVI shows a good relation with woody vegetation (Ling *et al.* 2009). The value of RVI is lower for sparsely deciduous forests as compared with that of deciduous forests due to the low volume scattering. However, RVI is very low for deforested area (0.17) because of the lower HV backscattering. Hence, RVI can be used for mapping of forest density and deforestation.

The estimated PH is shown in Figure 14. The mean value of PH is observed to be higher for evergreen, (0.41) medium for deciduous (0.26) and sparsely deciduous (0.20) forests, and lower (0.04) for the deforested area (Figure 15). PH gives a good contrast between different types of forest cover. The high value of PH indicates more un-polarized scattering components in the received signals and the presence of multiple scattering mechanisms. PH is a good parameter for differentiating the types of the forests and the deforested area.

Figure 16 shows the R:G:B colour composite of the Freeman–Durden decomposition. It gives realistic and detailed information about the types of scattering mechanisms for various scatterers and provides the percentage of even, odd and double bounce scattering mechanisms occurring in the study area. The evergreen forest shows a higher value of volume scattering (0.43) compared with the deciduous (0.42) and the sparsely deciduous (0.31) forests. In contrast, the evergreen forest shows a low value of surface (0.03) and double bounce scattering (0.01), whereas deciduous and sparsely deciduous forests show a high value (Figure 17 and Table 3). The deforested area shows a very low value of the volume (0.04) and double bounce (0.01) scattering and high for surface scattering (0.25). High volume scattering in evergreen forest is because of the multi-story tree structure with complex canopy (Guerra *et al.* 2008).

5. Conclusion

Characterization of the forests and deforestation in Cambodia have been made using the full polarimetric PALSAR by observing the backscattering coefficients (σ°), H , α , A , PH, RVI and Freeman–Durden three-component decomposition parameters. These properties depend on the interaction of PALSAR signal with forest types. The mean σ° HV observed for evergreen, deciduous, sparsely deciduous and deforestation were -12.96 , -12.99 , -14.29 and -22.25 dB, respectively. The deciduous forests have shown the value of σ° HV close to evergreen forest may be because of the saturation of PALSAR signal at 100 tons/ha as noticed by Watanabe *et al.* (2006). The value of mean σ° HV is very low for deforested area due to the absence of volume scattering. The observed entropy and RVI were highest for evergreen forest and lowest for the deforested area, whereas the pattern was reverse for HH/HV polarization ratio. Freeman–Durden decomposition shows high volume scattering in forested area, whereas surface scattering contribute in deforested area. Our observation shows that σ° HV, cross-polarization ratio (HH/HV), H and RVI give better results for the characterization of forest types and deforested area as compared with other polarimetric parameters.

Acknowledgements

The authors are highly thankful to the Monbukagakusho (MEXT) Japanese Government Fellowship to pursue the research at the University of Tokyo, Japan. The authors also want to emphasize the contribution of the Institute of Industrial Science, The University of Tokyo, for facilitating the data analysis in its laboratories and also to the Department of Civil Engineering, The University of Tokyo and Global Centers of Excellence (GCOE Program) for providing the requisite fund during the field visits.

References

- Achard, F., *et al.*, 2010. Estimating tropical deforestation from earth observation data. *Carbon Management*, 1 (2), 271–287.
- Avtar, R., Takeuchi, W., and Sawada, H., 2011. Full polarimetric PALSAR-based land cover monitoring in Cambodia for implementation of REDD policies. *International Journal of Digital Earth*. DOI: 10.1080/17538947.2011.620639.
- Beaudoin, A., *et al.*, 1994. Retrieval of forest biomass from SAR data. *International Journal of Remote Sensing*, 15 (4), 2777–2796.
- Cloude, S.R. and Pottier, E., 1997. An entropy based classification scheme for land applications of polarimetric SAR. *IEEE Transactions on Geoscience and Remote Sensing*, 35 (1), 68–78.
- Dobson, M.C., *et al.*, 1995. Estimation of forest biophysical characteristics in northern Michigan with SIR-C/X-SAR. *IEEE Transactions on Geoscience and Remote Sensing*, 33 (4), 877–896.
- Fang, C., Wen, H., and Yirong, W., 2006. An improved Cloude-Pottier decomposition using H/α /SPAN and complex Wishart classifier for polarimetric SAR classification. *In: CIE06, international conference on Radar*, Shanghai.
- FRA, 2005. *Global forest resources assessment*. Rome: Food and Agriculture Organisation of the United Nations.
- FRA, 2010. *Global forest resources assessment*. Rome: Food and Agriculture Organisation of the United Nations.
- Freeman, A. and Durden, S.L., 1998. A three-component scattering model for polarimetric SAR data. *IEEE Transactions on Geoscience and Remote Sensing*, 36, 963–973.
- Gardner, T.A., *et al.*, 2009. Prospects for tropical forest biodiversity in a human-modified world. *Ecological Letters*, 12, 561–582.
- Gibbs, H.K. and Herold, M., 2007. Tropical deforestation and greenhouse gas emissions. *Environmental Research Letters*, 2 (4), 1–3.

- Gibbs, H.K., *et al.*, 2007. Monitoring and estimating tropical forest carbon stocks: making REDD a reality. *Environmental Research Letters*, 2 (4), 1–13.
- Guerra, J.B., Freitas, C.D.C., and Mura, J.C., 2008. Evaluating potential of band polar data to discrimination increment areas in Amazon rain forest. *In: Proceedings of IEEE IGARSS08*.
- IPCC, 2007. *The physical science basis: summary for policymakers*. Intergovernmental Panel on Climate Change.
- Kim, Y. and van Zyl, J., 2001. Comparison of forest estimation techniques using SAR data. *In: Proceedings of IGARSS2001*.
- Kiyono, Y., *et al.*, 2010. Carbon stock estimation by forest measurement contributing to sustainable forest management in Cambodia. *Japan Agricultural Research Quarterly*, 44 (1), 81–92.
- Knuth, R., *et al.*, 2009. Multisensor analysis for forest monitoring in boreal and tropical forest environments. *In: Proceedings of IEEE IGARSS09*.
- Kuntz, S., 2010. Potential of spaceborne SAR for monitoring the tropical environments. *Tropical Ecology*, 51 (1), 3–10.
- Isoguchi, O., Shimada, M., and Uryu, Y., 2009. A preliminary study on deforestation monitoring in Sumatra island by PALSAR. *In: Proceedings of IEEE, IGARSS 09*.
- Lackey, R.T., 1998. Seven pillars of ecosystem management. *Landscape and Urban Planning*, 40, 21–30.
- Le Toan, T., *et al.*, 1992. Relating forest biomass to SAR data. *IEEE Transactions Oil Geoscience and Remote Sensing*, 30, 403–411.
- Lee, J.S. and Pottier, E., 2009. *Polarimetric radar imaging: from basics to application*. Boca Raton: CRC Press, Taylor and Francis Group.
- Ling, F., Chen, Z., and Wang, Q., 2009. Comparison of ALOS PALSAR RVI and Landsat TM NDVI for forest area mapping. *In: IEEE, APSAR 2009*.
- Lu, D., 2006. The potential and challenge of remote sensing-based biomass estimation. *International Journal of Remote Sensing*, 27 (7), 1297–1328.
- Mitchard, E.T.A., *et al.*, 2009. Using satellite radar backscatter to predict above-ground woody biomass: a consistent relationship across four different African landscapes. *Geophysical Research Letters*, 36, L23401. doi:10.1029/2009GL040692.
- Qi, Z., *et al.*, 2010. Land use and land cover classification using RADARSAT-2 polarimetric SAR image. *International Archives of Photogrammetry and Remote Sensing*, XXXVIII (part 7A), 198–203.
- Ramankutty, N., *et al.*, 2007. Challenges to estimating carbon emissions from tropical deforestation. *Global Change Biology*, 13, 51–66.
- REDD, 2010. Source book. GOF-C-GOLD [online]. Available from: <http://www.gofc-gold.uni-jena.de/redd/> [Accessed 17 January 2010].
- Rudel, T.K., *et al.*, 2009. Changing drivers of deforestation and new opportunities for conservation. *Conservation Biology*, 23 (6), 1396–1406.
- Schrope, M., 2009. When money grows on trees. *Nature Reports Climate Change*, 3, 101–103.
- Shimada, M., *et al.*, 2009. PALSAR polarimetric calibration and geometric calibration. *IEEE Transactions on Geoscience and Remote Sensing*, 47 (12), 3915–3932.
- Trisasonkko, B.H., 2010. The use of polarimetric SAR data for forest disturbance monitoring. *Sensing Imaging*, 11 (1), 1–13.
- Watanabe, M., *et al.*, 2006. Forest structure dependency of the relation between L-band σ° and biophysical parameters. *IEEE Transactions on Geosciences and Remote Sensing*, 44 (11), 3154–3165.
- Werf, G.R., *et al.*, 2009. CO₂ emissions form forest loss. *Nature Geoscience*, 2, 737–738.